Tectonophysics 627 (2014) 108–121

Contents lists available at ScienceDirect

Tectonophysics

journal homepage: www.elsevier.com/locate/tecto

Moho depth, seismicity and seismogenic structure in China mainland

Jiwen Teng [a,*], Yangfan Deng [a,b], José Badal [c], Yongqian Zhang [a]

[a] State Key Laboratory of Lithospheric Evolution, Institute of Geology and Geophysics, Chinese Academy of Sciences, Beijing 100029, China
[b] Guangzhou Institute of Geochemistry, Chinese Academy of Sciences, Guangzhou 510640, China
[c] Physics of the Earth, University of Zaragoza, Pedro Cerbuna 12, 50009 Zaragoza, Spain

ARTICLE INFO

Article history:
Received 3 July 2013
Received in revised form 5 September 2013
Accepted 3 November 2013
Available online 13 November 2013

Keywords:
Moho depth
Earthquake hypocenters
Seismic energy
Seismogenic layer
East Asia

ABSTRACT

The study of the crust–upper mantle structure based on wide-angle seismic profiles performed in China mainland since 1958, has provided tighter constraints on the architecture and deformation of the lithosphere; but the link between the seismic velocity structure and the seismogenic layer of the crust is still an open problem in which we are particularly interested. Starting from the crustal P-wave velocity models obtained along numerous seismic profiles, we have mapped the Moho depth beneath East Asia. The results demonstrate that the average Moho depth is about 35 km in Southeast China, 38 km in North and Northeast China, 51 km in Northwest China and 65 km in Tibet. The Moho depth varies between 20 and 28 km in the continental margin and sea area. Most of the earthquakes in China mainland have magnitude lower than 4.0 and generally occur in the uppermost 20 km of the crust and therefore above the Moho discontinuity; the average focal depth is found at 10 km in Southeast China, 12 km in North and Northeast China, 15 km in Northwest China and 13 km in the Tibetan Plateau. The ratio of the average focal depth to the Moho depth is approximately 0.3. Taking the lower bound of the natural seismicity as the depth above which is located 90% of the foci of earthquakes, we have found this limit at depths of 21, 41, 30 and 36 km in each of the mentioned blocks, respectively. In North and Northeast China some earthquakes occur below the Moho (at 41 km depth on average versus 38 km), although the average focal depth observed here is of only 12 km. Once defined the seismogenic layer as the layer that concentrates 80% of the released seismic energy, we have found that the difference in seismic velocity with respect to the other two crustal layers which extend above and below varies from 0.1 to 0.9 km/s in East Asia. This finding enables to discriminate the place with greater or lesser capacity to generate seismic energy. A difference in seismic velocity bigger than 0.9 km/s would mean that the layer has an earthquake generating capacity lesser than the seismogenic layer, as greatly happens in South China and Northwest China; while a smaller velocity difference would imply that the layer has a comparable seismogenic capacity, as happens in Tibet.

1. Introduction

Special attention has been paid to several topics (the spatial variation of the Moho depth, the deep structure of the crust, the seismicity pattern, etc.) related to the tectonic and geodynamics in very different areas of the world. These issues have been addressed through a series of research projects which have provided important geophysical, geochemical and geological information. As examples, we cite some works that have contributed to get accurate images of the Moho depth and the structure of the earth crust in western North America (Gorman et al., 2002), South America (Lloyd et al., 2010), Europe (Grad and Tiira, 2009) and eastern Asian continent (Teng et al., 2003). But at least in China the link between the seismic velocity structure and the seismogenic layer of the crust is still an open problem that we want to tackle in this study.

The crustal thickness in China has been mapped from gravity data and deep seismic soundings (DSS) performed in the last years. Although the gravity data are usually affected by the undulating geometry of the topographic relief and the different accuracy of the field measurements made in the course of geophysical surveys during different time periods, such data have helped to investigate the crustal thickness in those regions with lack of seismic data (Chen et al., 2001; Deng et al., 2013; Feng, 1985; Wang, 1985; Zhu et al., 1996). Recently, the Moho depth in East Asia has been investigated from quality DSS data (specifically Pm and Pn seismic phases) by block modeling and segmentally interactive ray tracing (Xu et al., 2006, 2010) with precision of ±1 km (Teng et al., 2003). Recognizing the merit of pioneer works (Liu et al., 1994; Song et al., 1994; Teng et al., 1982; Yin et al., 1990), the mapping of the Moho discontinuity has contributed to obtain valuable information on the deep structure of the crust and thereby about the tectonics and continental dynamics in East Asia (Li et al., 2006, 2013; Prodehl et al., 2013; Teng et al., 2003, 2013; Thybo and Artemieva, 2013; Yang et al., 2013; Zhang et al., 2005, 2011c).

The focal mechanism and the focal depth of the earthquakes are some of the most accessible indicators to study its origin and the mechanical properties of the lithosphere (Teng et al., 2003); together with the magnitude and released energy are the basic elements to

* Corresponding author.
E-mail address: jwteng@mail.iggcas.ac.cn (J. Teng).

0040-1951/$ – see front matter © 2013 Elsevier B.V. All rights reserved.
http://dx.doi.org/10.1016/j.tecto.2013.11.008

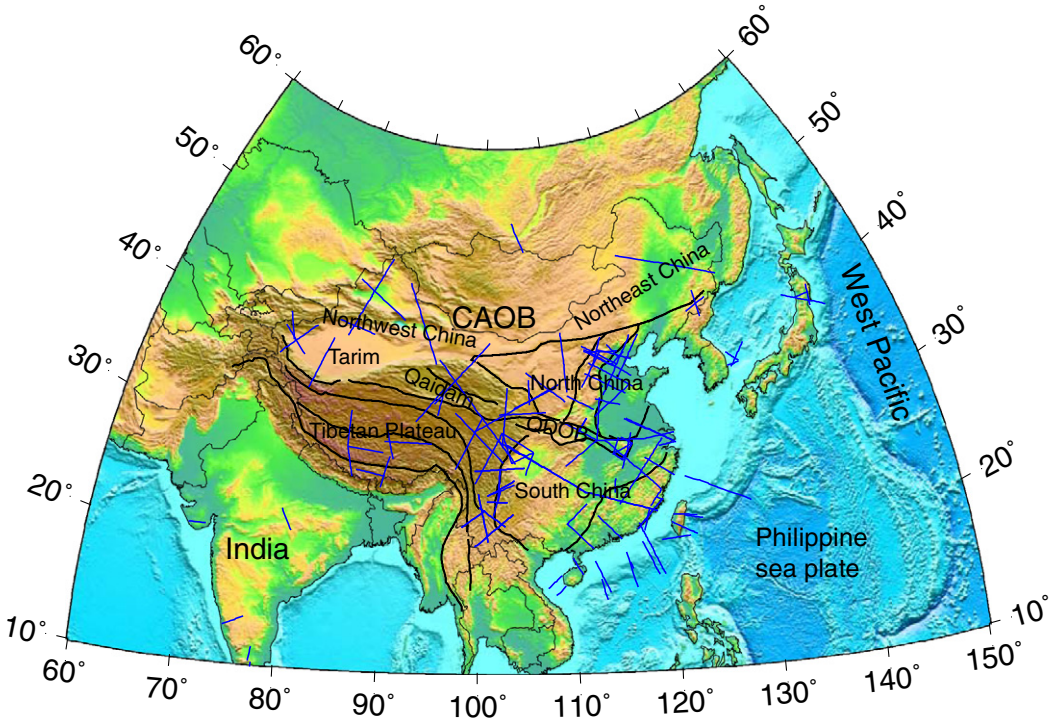

Fig. 1. Major tectonic regions considered in this study: Southeast China, North and Northeast China, Northwest China and Tibetan Plateau. Key to symbols: CAOB, Central Asian orogenic belt; QDOB, Qinling–Dabie orogenic belt. The solid black lines stand for tectonic boundaries; blue straight lines represent deep seismic profiles performed in East Asia during the period 1974–2010 (a detailed description can be seen in Teng et al., 2013).

analyze the rheology of the crustal lithosphere and its seismogenic structure (Foster and Jackson, 1998; Maggi et al., 2000; Molnar and Chen, 1983; Zhang et al., 2013a). For example, the earthquake occurrence in an active plate margin presents very significant features of these elements besides a characteristic bias consisting in a foci clustering with progressive tilt as the depth increases, what led to the

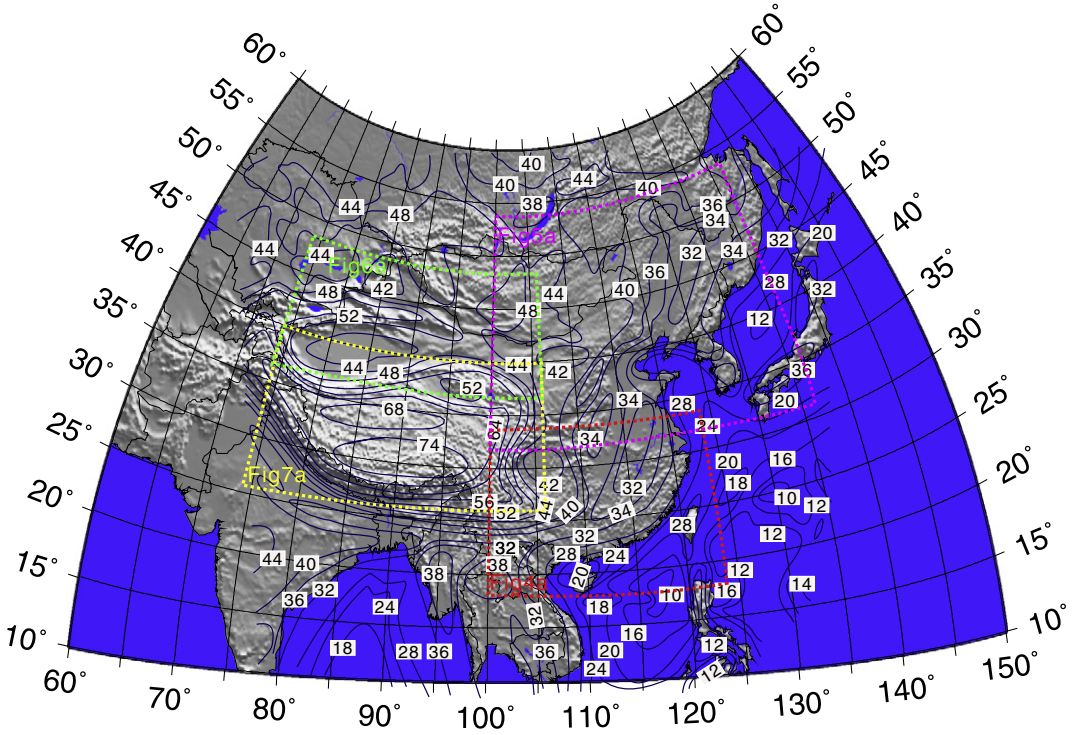

Fig. 2. Mapping of the Moho depth in East Asia (the values associated to isolines both inland and offshore indicate depth in km). The areas to which we refer in Figs. 3a, 4a, 5a and 6a are delimited by contour lines.

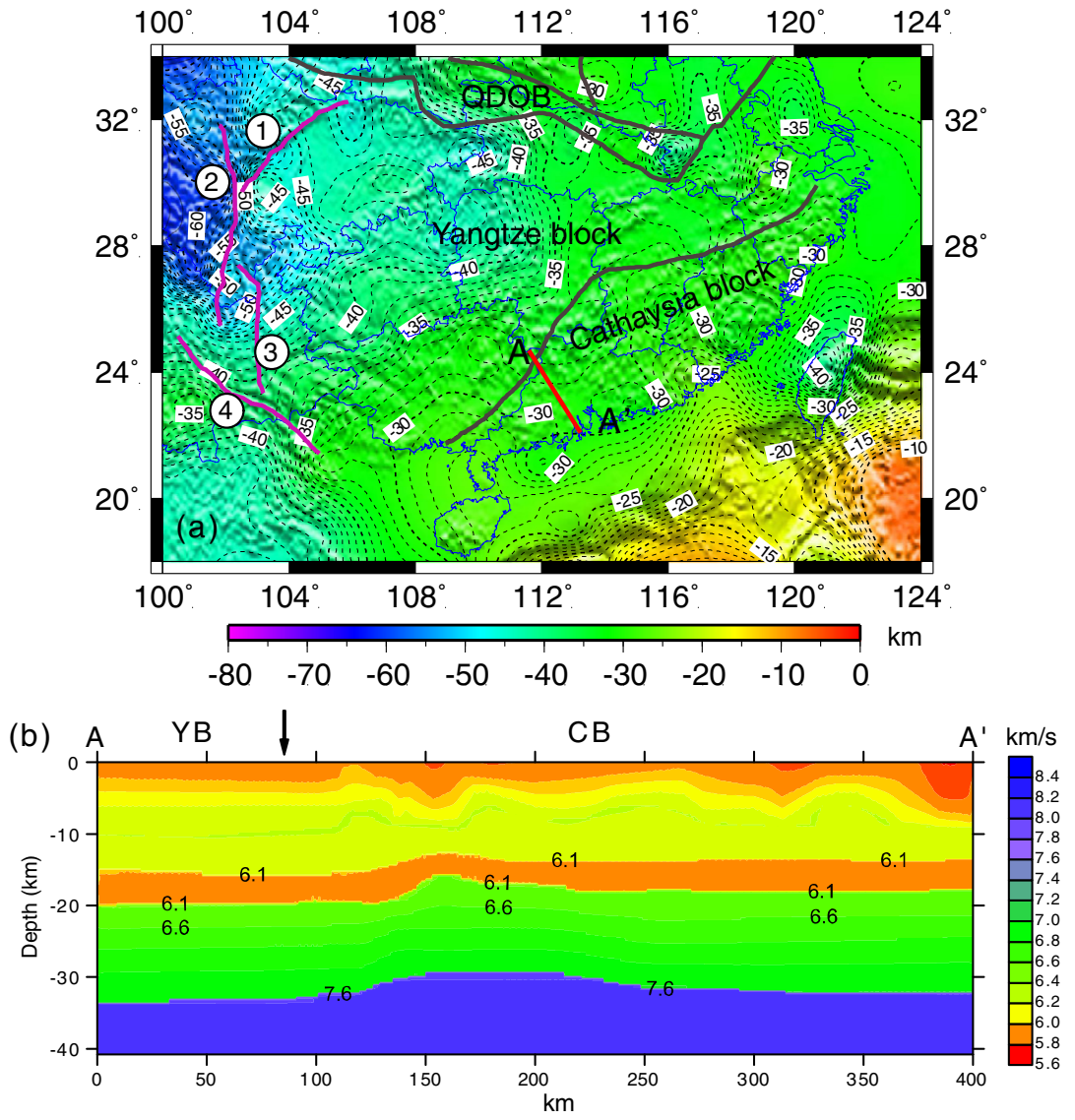

Fig. 3. (a) The Moho depth in South China; the brown lines stand for the tectonic boundaries; the purple lines to the west depict faults: ①: Longmenshan fault; ②: Xianshuihe fault; ③: Xiaojiang fault; ④: Red River fault. (b) P-wave velocity section along the Lianxian–Gangkou profile (transect AA' in the above plot). The Wuchuan–Sihui fault that is the crustal-scale feature that defines the boundary between the Yangtze block and the Cathaysia block is marked by an arrow on the top. Acronyms: QDOB, Qinling–Dabie orogenic belt; YB, Yangtze block; CB, Cathaysia block.

concept of subduction zone and has played a key role in plate tectonics. However, when compared with plate boundary earthquakes, the intraplate earthquakes, as is the case in East Asia, pose a more complicated problem since the determination of source parameters is constrained by many factors, such as network station density and its spatial distribution (coverage) and the knowledge of the local structure of the crust.

The study region (10ºN–60ºN, 70ºE–140ºE) includes a great part of the Asian continent, the eastern continental margin and the near oceanic area of West Pacific (Fig. 1). In this paper, we present the map of the Moho depth based on the results provided by numerous deep seismic soundings performed in this large area. Then, after a brief review of the focal mechanisms, focal depths and magnitudes of the regional earthquakes, we analyze the relationship between seismicity and Moho depth with respect to the major tectonic units that make up the study region. Finally, we make reference to the seismogenic structure of the crust by contrasting the seismogenic layer with the other two layers extending above and below, which helps to understand the earthquake generation capacity in the different blocks in which we have divided East Asia.

2. Implementation

Since the pioneer experiments based on deep seismic surveys and performed in Qaidam basin in 1958 (Teng, 1979; Zeng and Gan, 1961), numerous seismic profiles with a total length of 60,000 km (including seismic reflection profiles deployed on over 10,000 km) have been conducted to date by the Chinese Academy of Sciences, Chinese Seismological Bureau and the Ministry of Lands and Resources of China. The geographical location of these wide-angle seismic profiles is certainly uneven. The coverage is relatively good in the North China Craton, South China and the Tibetan Plateau, with the exception of northeastern China and the western part of Tibet (Fig. 1). Some deep seismic soundings extend over adjacent oceanic areas; however, some of their results are not published yet and therefore are unavailable for our study. In some zones there are too many overlapping profiles and the contrary happens in other ones, so that a careful selection and processing of data is needed.

In the areas poorly covered by observational data, we used weighted interpolation controlled by sufficient data points to ensure the reliability

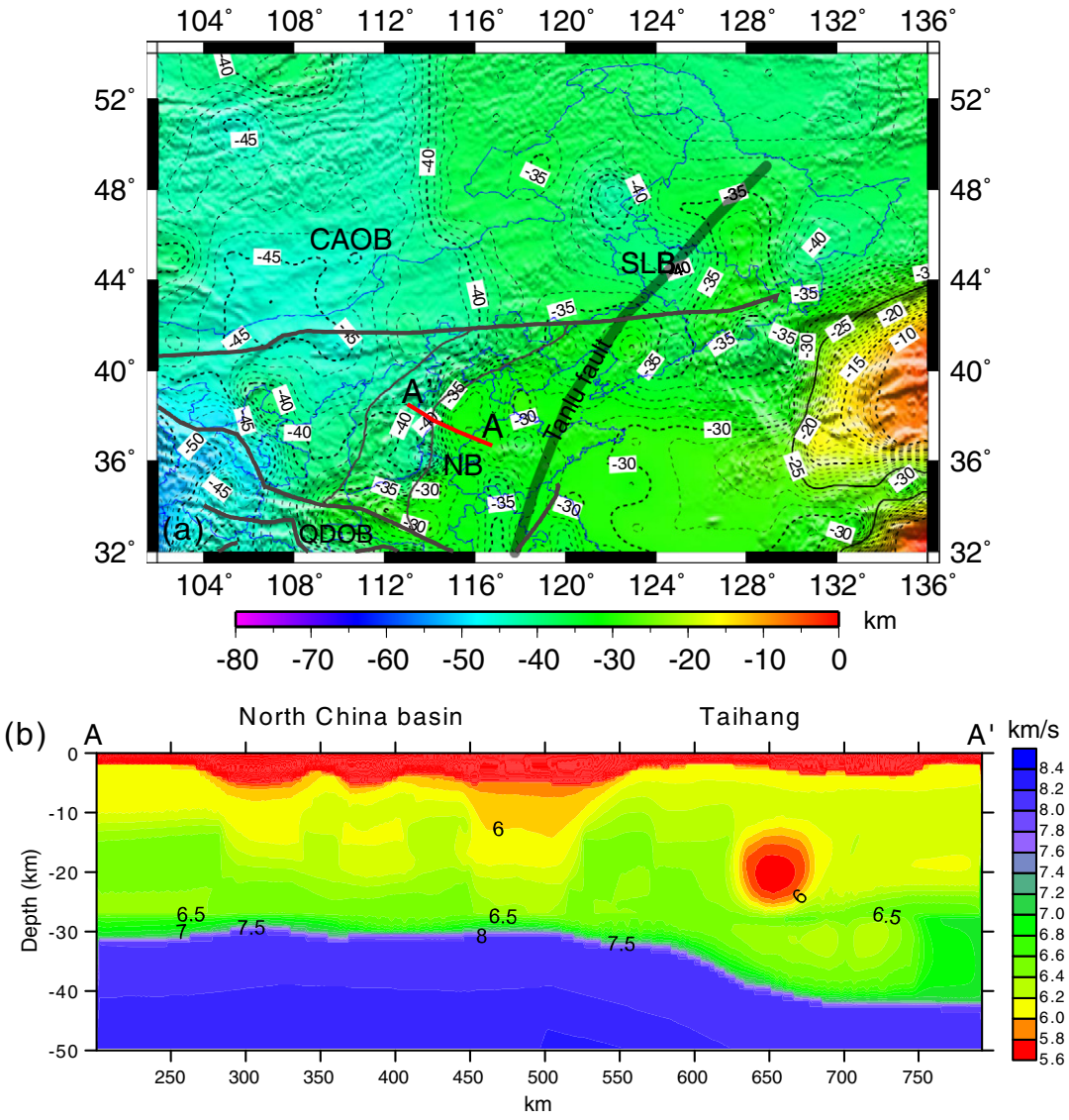

Fig. 4. (a) The Moho depth in North and Northeast China; the brown lines stand for tectonic boundaries. (b) P-wave velocity section along the Yingxian–Zibo profile (transect AA′ in the above plot). Acronyms: CAOB, Central Asian orogenic belt; SLB, Songliao basin; NB, North China basin; QDOB, Qinling–Dabie orogenic belt.

of the final result. At those zones where the data overlap and show discrepancy, we selected the information taking into consideration the coherence with the data from surrounding areas. On the southern margin of East Asia, especially in the oceanic regions where seismic sounding data are insufficient or non-existent, we have taken the results of the Crust 2.0 model (Laske et al., 2001).

Despite these drawbacks, we have collected abundant information, perfectly compiled until 2010, which provides an updated database for mapping the Moho undulation and the seismic velocity structure of the crust in most part of China mainland.

3. Moho depth distribution in East Asia

The map shown in Fig. 2 is the result of the last compilation of data supplied by deep seismic profiles performed in China. This map is an updating of previous results obtained from different data sources and methods (Teng et al., 2013; Zhang et al., 2011c), and gives accurate data about the crustal thickness within the spatial window (10ºN–60ºN, 70ºE–140ºE). As expected, the Moho depth varies roughly between 10 and 75 km in East Asia, and is different beneath the continent (32–75 km) and the ocean (10–28 km). Broadly, the crustal thickness undergoes a remarkable thinning west-to-east even from north to south with the exception of the Tibet Plateau. The isolines describing the Moho depth present a clear NNE–SSW trend in the east, but E–W in the west, in agreement with the main tectonic trends in the continental domain (Ma, 1989). Taking as tectonic references the north–south tectonic belt and the Central Asian orogenic belt formed by the Qinling–Dabie and Kunlun orogens (Zhang et al., 2013a), and without losing sight the constraints affecting the distribution of the seismic activity with especial attention to focal mechanism, focal depth and magnitude, the study area can be divided into four parts, namely: Southeast China, North and Northeast China, Northwest China, and Tibetan Plateau (Fig. 1). With relation to this partition, the Moho depth is 35 ± 5 km in Southeast China, 30–45 km in North and Northeast China, 20–28 km in the continental margin and sea area, 44–48 km in Northwest China (around 48 km in Tarim basin), and 75 km or more in the Tibetan Plateau where the crust reaches its maximum thickness (Fig. 2). Below we highlight some results concerning the Moho depth and crustal seismic velocities for each of the mentioned domains.

3.1. Southeast China

This region, sometimes simply called South China, is an important part of the tectonic framework of the continental margin of East Asia.

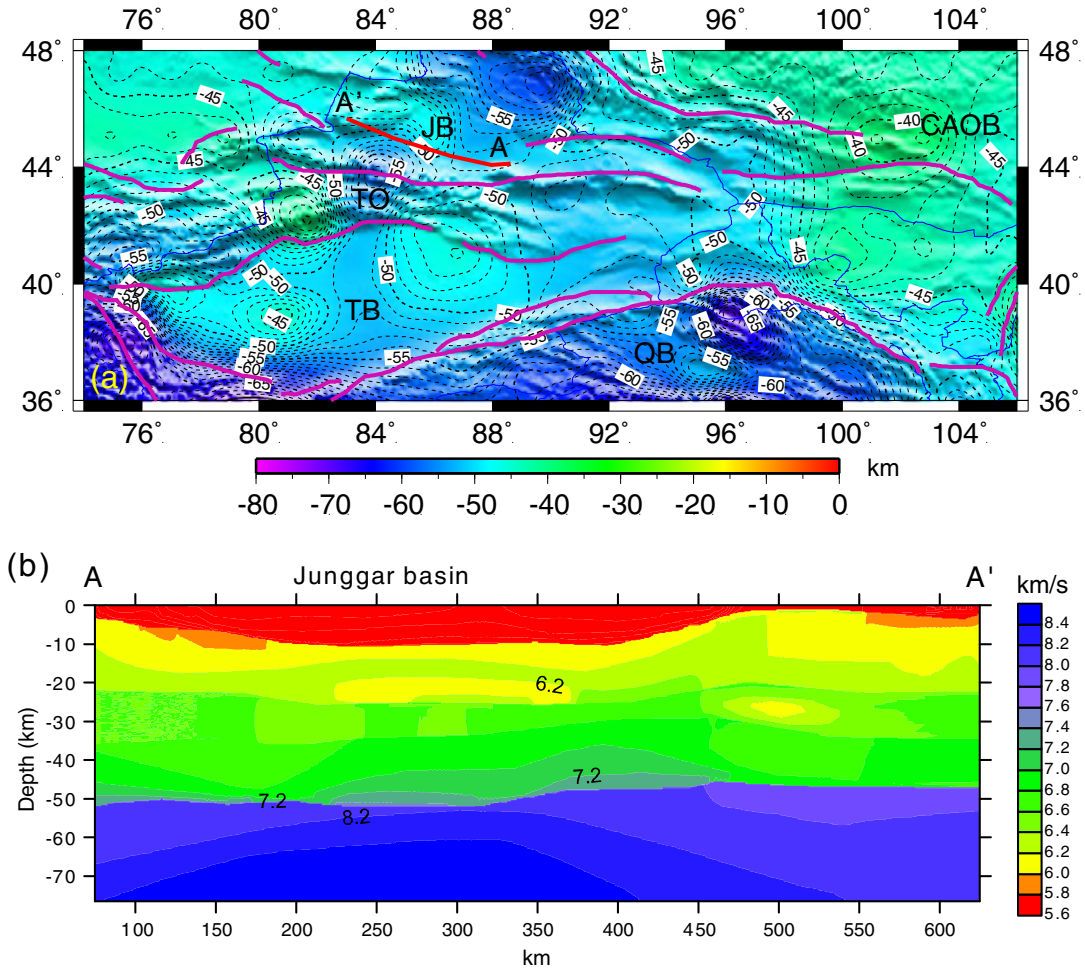

Fig. 5. (a) The Moho depth in Northwest China; the purple lines depict faults. (b) P-wave velocity section along the Qitai–Emin profile (transect AA′ in the above plot). Acronyms: JB, Junggar basin; TO, Tianshan orogen; TB, Tarim basin; QB, Qaidam basin; CAOB, Central Asian orogenic belt.

The South China block is commonly divided into two major tectonic blocks (Fig. 3a): the Yangtze craton to the northwest and the Cathaysia or Huanan block to the southeast (Li, 1994; Zhang et al., 1984; Zhao and Cawood, 1999). Recently, Wang et al. (2013) have posed interesting observations and controversies about the Phanerozoic tectonics of the South China block. A recent comprehensive review about the formation and evolution of the Precambrian continental lithosphere in South China can be seen in Zhang and Zheng (2013).

The Moho is deeper than 30 km everywhere in the continent, and the crust is remarkably thicker in the west than in the east. The Sichuan basin has a relatively flat Moho whose depth reaches approximately 42 km. The Moho in the continental margin and sea area has a less depth around 20–28 km.

In order to illustrate the P-wave velocity structure of the crust in South China, we have constructed a section along the 400-km-long Lianxian—Gangkou Island profile (Yin et al., 1999; Zhang and Wang, 2007). This profile (Fig. 3b) crosses the Yangtze and Cathaysia blocks and the Wuchuan–Sihui fault that is the crustal-scale feature that defines the boundary between these two blocks (Zhang et al., 2008, 2009, 2011c, 2012; Zhao et al., 2013a, 2013b). As can be seen, the sedimentary cover extends above an upper layer with P-wave velocity between 6.0 and 6.15 km/s. Such as deep seismic reflections and Moho seismic refractions clearly reveal, the P-wave velocity increases quickly to 6.5–6.6 km/s immediately below the thin middle crust, to become 6.7–6.8 km/s in the upper half of the lower crust and 7.6 km/s at the bottom (Zhang and Wang, 2007). The lower crust is about 13 km thick and exhibits no strong lateral variation in velocity. There is a thin low-velocity layer (P-wave velocity of 5.8 km/s) with only 5 km of thickness in the middle crust. Two explanations can be advanced for this layer. The first one is that this low velocity zone is a ductile shear zone (Zhou and Li, 2000), and the presence of hot springs at surface could be due to this ductile shear zone or body of high heat conductivity. The second explanation is that the low velocity layer has been strongly altered by the presence of partially molten rock (Zhang and Wang, 2007).

3.2. North and Northeast China

The North China block is one of the oldest continental nuclei in the world (Jahn and Nyquist, 1976) and consists of two Archean blocks: the western block and the eastern block with reported crustal ages of 3.8 Ga (Liu, 1992), which are separated by a Paleoproterozoic orogenic belt of 1.8 Ga (Santosh et al., 2010, 2012; Zhai et al., 2007; Zhao et al., 2001, 2003). Located between the Siberian craton and the North China craton (Jahn et al., 2000; Sengör and Burtman, 1993; Sengör et al., 1996; Xiao et al., 2003, 2004), Northeast China has been traditionally considered as the eastern segment of the Central Asian orogenic belt (Fig. 4a).

The crust reaches a depth of ~35–45 km and becomes thinner as we go to the east, being the Moho depth ~35 km on the eastern side of the Tanlu fault and only 26 ± 2 km in Bohai Bay (Fig. 4a). As before, to illustrate the P-wave velocity structure of the crust in the northeast

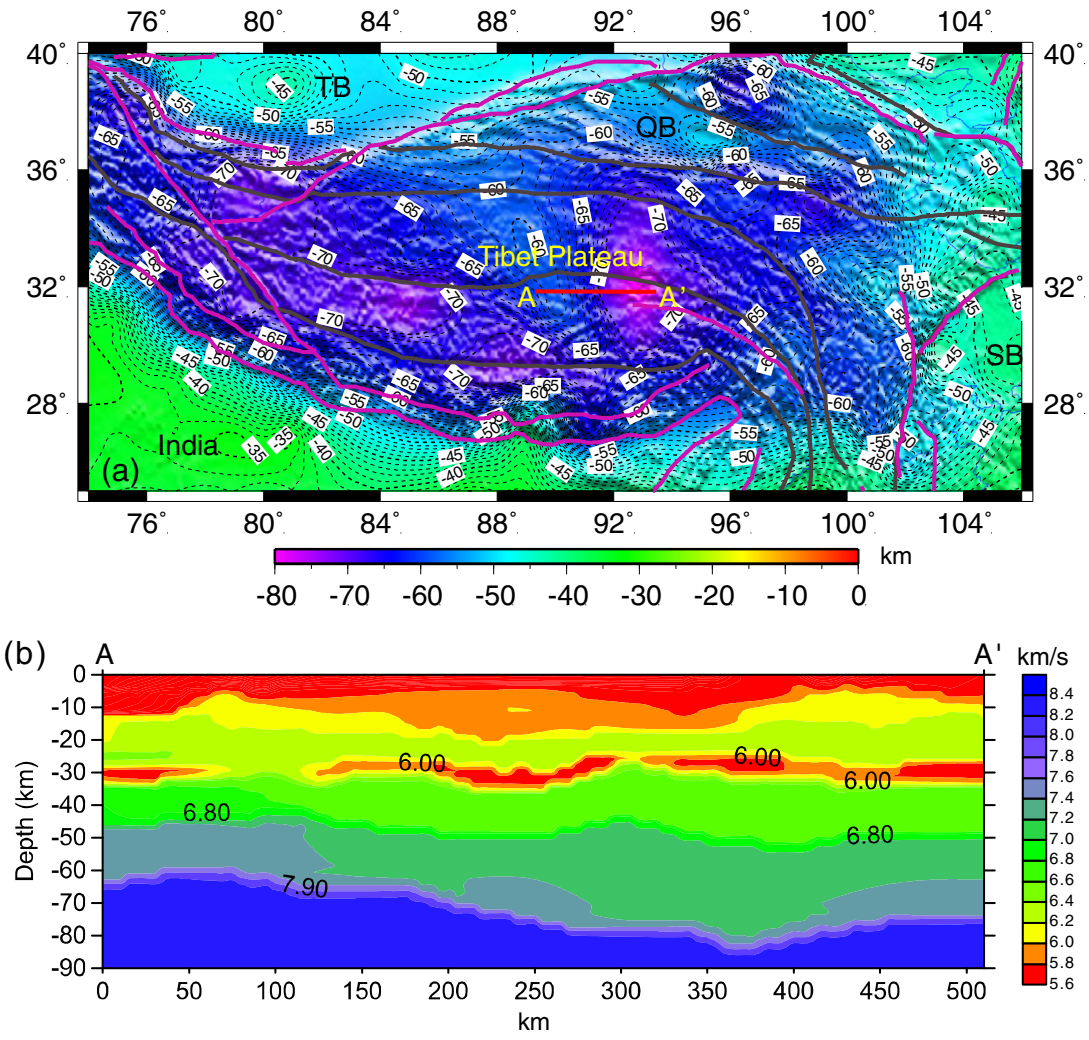

Fig. 6. (a) The Moho depth in Tibet; the purple lines depict faults. (b) P-wave velocity section along the Selin Tso–Yaando profile (transect AA′ in the above plot). Acronyms: TB, Tarim basin; QB, Qaidam basin; SB, Sichuan basin.

quadrant of China, we have constructed a section along the 600-km-long Yingxian–Zibo profile (Liu et al., 1996) (Fig. 4b). The Moho depth is ~31 km in the North China basin and the deepest lower crust is featured by P-wave velocity of 7.5 km/s, which becomes 8.0 km/s in the top of the lithospheric mantle. The crust thickens rapidly southeastward across the Taihang Mountain, being the Moho depth ~43 km. A detail to be noted is a sphere-shaped low-velocity body that exhibits a so low velocity as 5.6–5.8 km/s and is found at 20 ± 4 km depth beneath Taihang; this body could be related to the partially molten rocks resulting from the deformation of the decoupled crust after thickening and uplifting (Jia and Zhang, 2005; Liu et al., 1996).

3.3. Northwest China

The most interior part of Central Asia includes Siberia, Kazakhstan and the northwest quadrant of China where the Junggar and Tarim basins are separated by the Tianshan orogen which extends from west to east (Xiao and Kusky, 2009), as shown in Fig. 5a. The Moho depth reaches 50 km in Tarim basin and somewhat more ~55 km in Junngar basin where the crust is relatively thicker. To the east, the Moho depth remains close to 50 km; but it increases up to 60 km in Qaidam basin. The 500-km-long Qitai–Emin profile (Xue et al., 2006) separating the Junggar basin from the Tianshan orogen allow us to illustrate the seismic velocity structure of the crust in a small part of the region, as shown in Fig. 5b. The depth of the sediment cover in Junggar basin could be up to 10 km. The Moho depth varies very little and remains around 50 km. In this case, the only detail to be highlighted is an elongated-shaped low-velocity body (6.1 km/s) below the upper crust, that could be formed by the intrusion of ultrabasic magma and to be the origin for oil and gas in the Junggar basin (Xue et al., 2006).

3.4. Tibetan Plateau

The Tibetan Plateau, which lies between the Kunlun Mts. and the Himalayas, occupies largely western China (Chang and Pan, 1981; Chang et al., 1986; Yin and Harrison, 2000; Zhang et al., 2011d, 2013b). Undoubtedly, it is the most outstanding and youngest example of continent–continent collision on Earth, and both the plateau and its neighboring regions are the ideal places for the study of the geological evolution of the Himalayan–Tibetan orogen (Yin and Harrison, 2000) and the lithospheric system in East Asia (Sherrington et al., 2004).

More than 23 DSS have been performed by the Chinese Academy of Sciences, often in international cooperation, in the 1970s, 1980s, 1990s and during the last years with the purpose of understanding the growth of the Tibetan Plateau (Cui et al., 1995; Gao et al., 2005; Li et al., 2001; Teng et al., 1981, 1983, 1985a, 1985b; Zhang et al., 2011b). To the

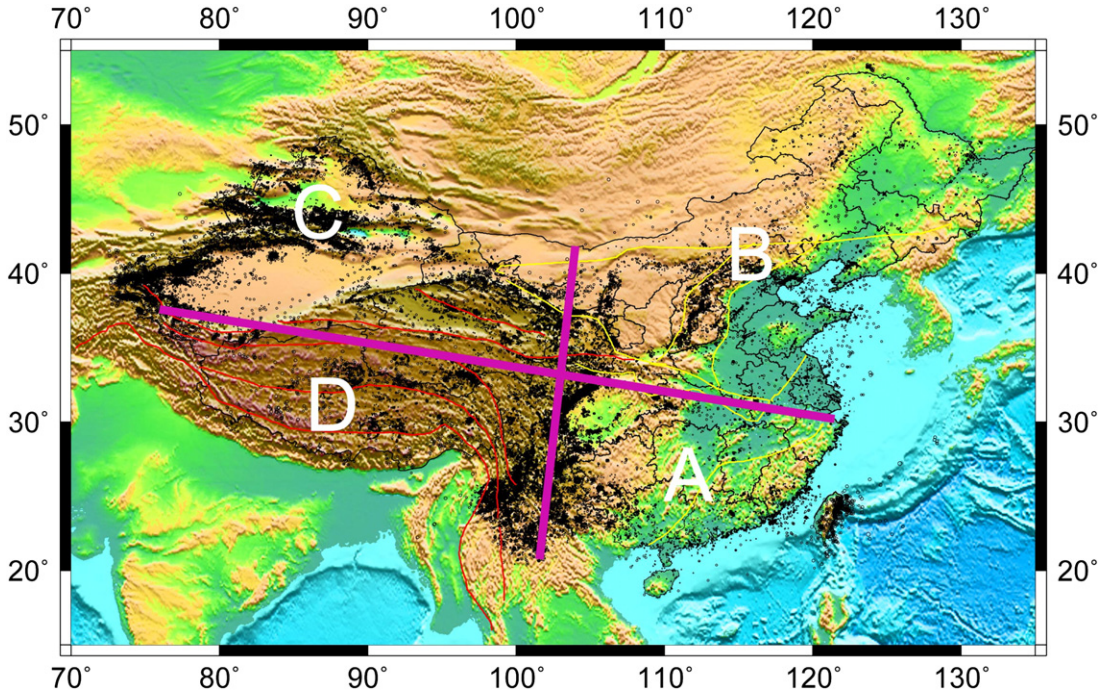

Fig. 7. Earthquakes occurred in China during the period January 2010-January 2013 (catalogued by the China Earthquake Network Center).

north of the plateau, the crustal thickness is some 50 km in Tarim basin and 60 km in Qaidam basin (Fig. 6a). The Moho beneath the Tibetan Plateau presents an undulating shape that lies between 60 and 73 km depth and reaches its maximum depth to the south. A clear correlation between the elevations of the Tibetan Plateau and the Moho topography suggests that a great part of the raised Plateau is isostatically compensated (Chen et al., 2009; Zhang et al., 2011c). The 510-km-long Selin Tso–Yaando profile (Zhang and Klemperer, 2005) allow us to illustrate the seismic velocity structure of the crust in this region (Fig. 6b). The crust can be roughly divided into an upper crust (5 to 30 km depth, $5.0 < Vp < 6.4$ km/s), middle crust (33 to 48 km depth, $6.5 < Vp < 6.8$ km/s) and lower crust (depths below 48 km, $7.1 < Vp < 7.4$ km/s). The Moho depth changes laterally from west to east, from 60 to 80 km. A low velocity layer (5.9 km/s) is observed at 30 km depth for then disappear westward; it might mean a region of incipient partial melting (Zhang and Klemperer, 2005).

4. Seismicity in China mainland

The national seismic network commonly uses the Geiger method (Geiger, 1912) for earthquake location, while the provincial seismic networks use the codes hypo2000 (Klein, 2002) and hypoDD (Waldhauser and Ellsworth, 2000). It is to be noted that the hypocentral determinations and especially the focal depth are affected by a certain degree of uncertainty due to the low density of seismic stations with which they are sometimes calculated. It is worth to be mentioned that the accuracy of the focal depth is still a thorny issue even today. In modern earthquake catalogs it has almost become one of the most inaccurate parameters. The accuracy in earthquake location is usually scaled as A, B, C or D, depending on whether the focal depth is determined with an uncertainty $\Delta \leq 5$ km, 5 km $< \Delta \leq 15$ km, 15 km $< \Delta \leq 30$ km, or $\Delta > 30$ km, respectively. According to the earthquake catalogs provided by the Chinese provincial networks, the lack of horizontal accuracy in the location of seismic events has 4 grades, namely: grade 1 corresponds to an error smaller than 5 km in epicentral location; grades 2, 3 and 4 correspond to 5 km < error < 15 km, 15 km < error < 30 km, and error > 30 km, respectively. The uncertainty in earthquake location with the help of the provincial networks refers only to epicentral location. It is not possible to determine the error in focal depth directly from the catalogs because of the relationship between error in the epicenter and error in depth (Zhang et al., 2011a). All these constraints should bear in mind when contrasting the seismicity in the different tectonic units.

All the seismic events collected in the Catalogue of the China Earthquake Network Centre (CENC) during the period 1 January 2010 — 1 January 2013, make a total of 158,752 earthquakes that are shown on a map in Fig. 7. Northwest China and the north–south tectonic belt (that also could be called north–south seismic belt because of its high seismicity) are the areas that comparatively have more earthquakes, while Southeast China and Northeast China and even the Tibetan Plateau have few earthquakes.

4.1. The focal mechanism in East Asia

The focal mechanism of an earthquake describes the inelastic deformation that happens in the source region and generates the seismic waves. Under the hypothesis of an event caused by a fault, its solution is called fault-plane solution and describes both the orientation of the fault plane where the slipping took place and the slip vector (Sipkin, 1994). Here we report on the focal mechanism of the earthquakes occurred since 1976 in East Asia, based on the systematic application of the centroid-moment-tensor (CMT) algorithm to long-period seismograms recorded at globally distributed seismographic stations (Ekström et al., 2012). The CMT method is based on the existing linear relationship between the six independent elements of the zero-order moment-tensor solution of an earthquake and the generated ground motion (Gilbert, 1971). A total of 999 focal spheres are shown in Fig. 8. The black spheres stand for thrust faults (Fig. 8a); the red spheres normal faults (Fig. 8b) and the green ones stand for slip faults (Fig. 8c).

There are not many earthquakes with calculated focal mechanism in South China because here the seismic events have commonly small

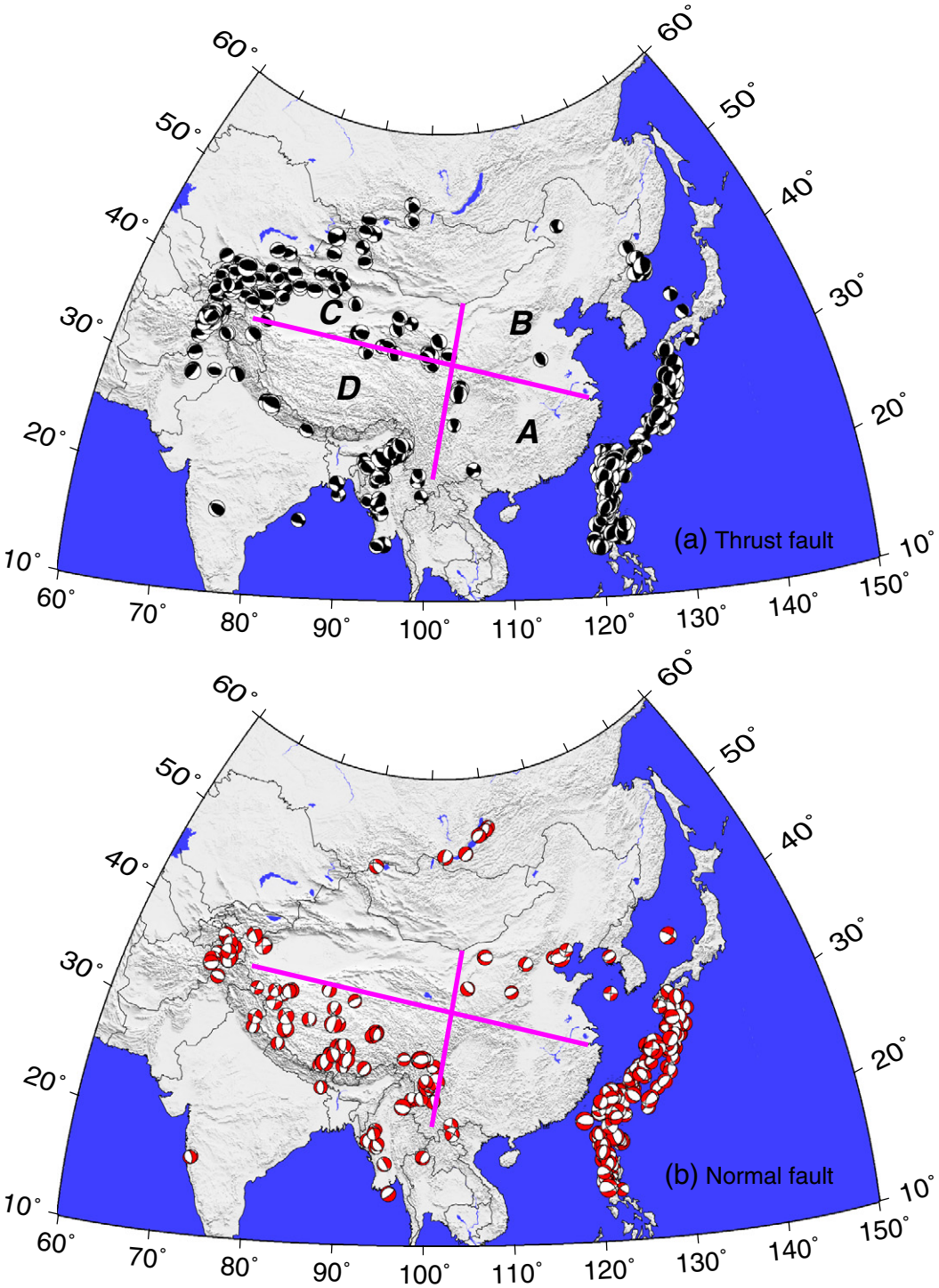

Fig. 8. Focal mechanism (fault-plane solution) of representative earthquakes (Ms > 5) occurred in East Asia since 1976: (a) thrust faults, (b) normal faults and (c) slip faults. A, Southeast China; B, North and Northeast China; C, Northwest China; D, Tibetan Plateau.

magnitude. Generally, North and Northeast China present normal fault mechanisms, which indicate that this wide region is dominated by extensional stresses. The thrust faults in Northwest China give the hint that this region is mainly subjected to a compression regime. Although the focal mechanisms around Tibet mainly correspond to thrust faults, the fact is that in the interior of Tibet such mechanisms describe normal faults; and further south, in Indo-China (southeast of Tibet), the fault-plane solutions mainly depict slip faults. The focal mechanisms bordering Tibet demonstrate that the margin of the plateau is under a convergent compressive regime, while the mechanisms of earthquakes in its interior indicate that Tibet is under an extensional stress regime.

4.2. Distribution of focal depths

In order to reduce as much as possible the error in focal depth and the uncertainty derived from unequal monitoring abilities at different places, we only have taken into account earthquakes with magnitude ML ≥ 2.0 recorded during the period 1980.01–2013.01. The earthquakes in each

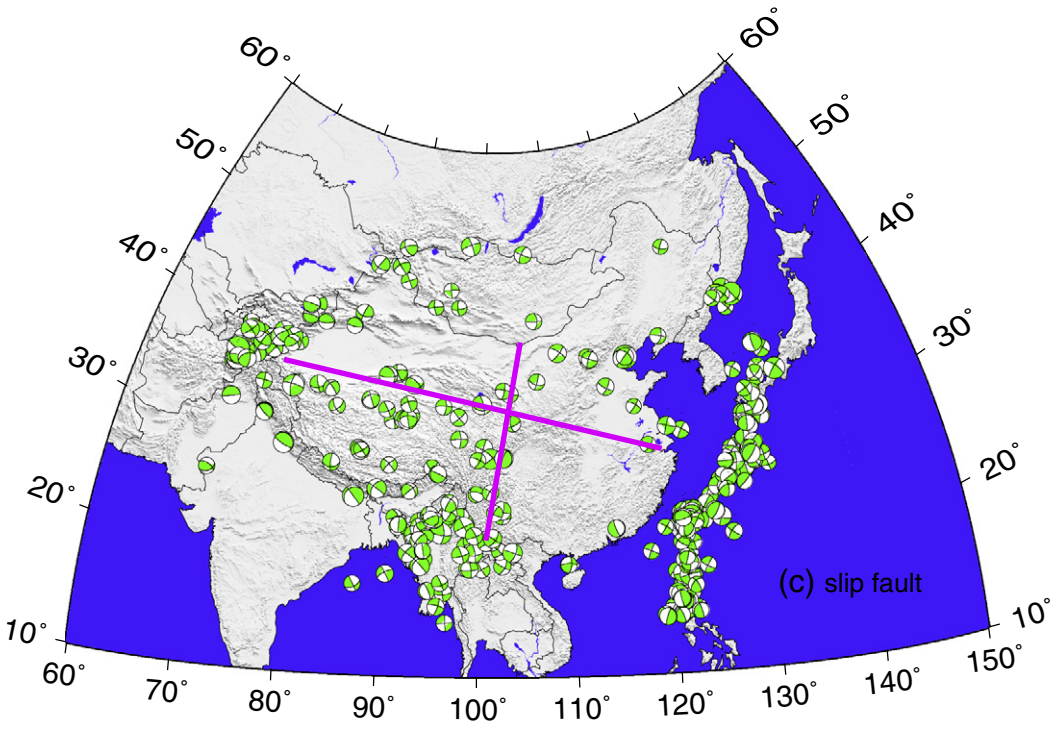

Fig. 8 (*continued*).

one of the four large tectonics units in which we have divided China mainland were counted at 4 km depth intervals. Given the small number of seismic events below 60 km depth, only those which are above this level were considered. Fig. 9 is a bar histogram showing focal depth versus number of earthquakes, thus allowing see at first glance the distribution of earthquakes in the four major large tectonic units of China. In South China most of the earthquakes are located in the upper crust at depths 4–12 km, and already in a less ratio at deeper depths; and the same happens in North and Northeast China where the earthquakes are found at depths 4–16 km, though clearly in a comparatively higher number at greater depths. In Northwest China the events are distributed within a somewhat larger depth range in the crust. The earthquakes in Tibet again occur mostly within a depth range 4–16 km, without excluding other events with greater focal depth.

4.3. Distribution of earthquake magnitudes

The distribution of magnitudes versus number of earthquakes is represented in Fig. 10. All the events exhibit the same features: the number of earthquakes decreases as its magnitude increases; almost all have magnitude that does not exceed 3.5–4.0 and are rare those having magnitude ML > 5.0. There are hardly earthquakes of magnitude above 6.5–7.0. Within a same magnitude range, South China is the region with the smallest amount of earthquakes.

4.4. Focal depth versus earthquake magnitude

To complete the frame of the seismicity in China mainland, in Fig. 11 we have correlated the magnitudes of the earthquakes with their respective focal depths. Although very gradually, the trend at a glance is

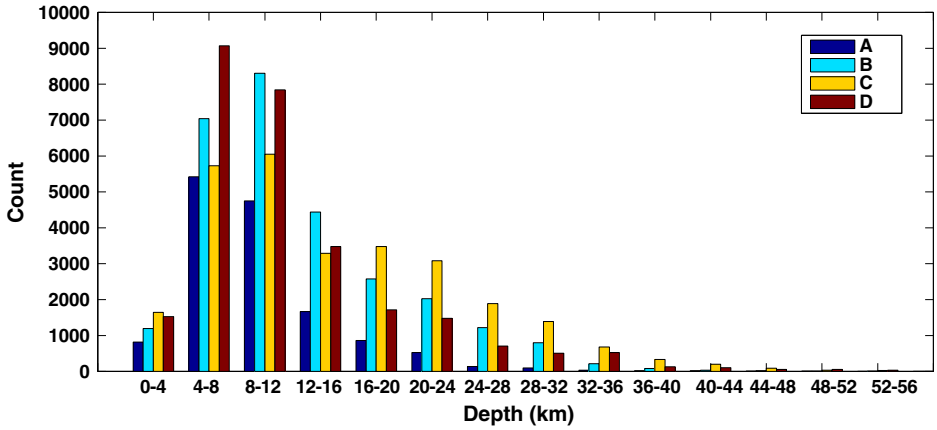

Fig. 9. Focal depth versus number of earthquakes. The data correspond to the earthquakes occurred during the period January 1980–January 2013. Key to columns: A, Southeast China; B, North and Northeast China; C, Northwest China; D, Tibetan Plateau.

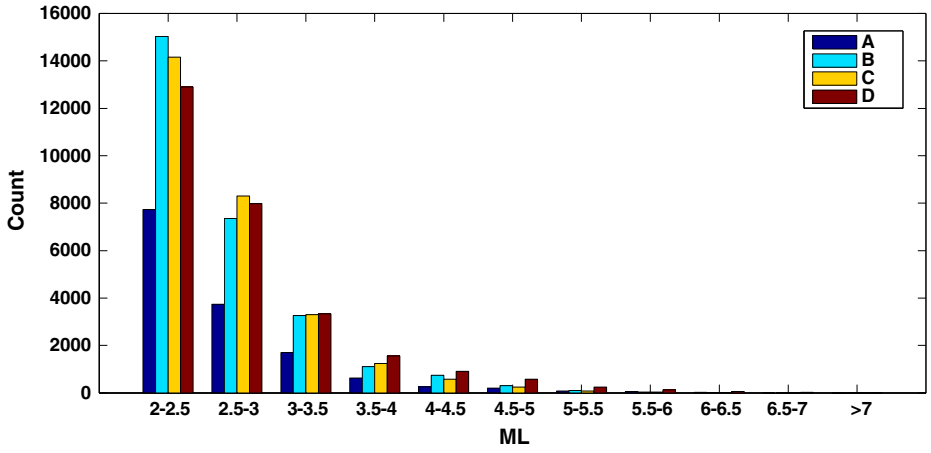

Fig. 10. Magnitude versus number of earthquakes. The data correspond to the earthquakes occurred during the period January 1980–January 2013. Key to columns: A, Southeast China; B, North and Northeast China; C, Northwest China; D, Tibetan Plateau.

that as the magnitude is bigger the depth is somewhat larger. Such as the histogram reflects, there are no earthquakes with ML > 7.0 in South China. All earthquakes are shallow with depths that generally do not exceed 20 km, except for North and Northeast China: here the more the magnitude ML > 5.0 is, the more the depth increases rapidly (with a gap for 6.5–7.0); even events with magnitude ML > 7.0 and focal depth over ~280 km have been detected. The big and deep earthquakes in North and Northeast China could be the combined result from the thrust of the Tibetan lithosphere and the subduction of the West Pacific (Lei and Zhao, 2005). Leaving aside large magnitudes and depths observed in the continental areas, the remaining characteristic is that the focal depth in Northwest China is a bit larger than in the other three tectonic regions.

5. Discussion

5.1. Relationship between seismicity and Moho depth

Numerous studies have demonstrated that the shallow seismic activity is concentrated at different depth ranges in different parts of the world. Molnar and Chen (1983) found that earthquakes which occur on continents are confined at the upper part of the crust, whose brittle nature ensures that earthquakes are relatively common here. Foster and Jackson (1998) provided evidence that earthquakes occur in the whole crust in East Africa, India, and Himalayas, although not below the Moho. Maggi et al. (2000) addressed issues such as focal depths, effective elastic thickness and the strength of the continental lithosphere. More recently, Zhang et al. (2011c, 2013a) have illustrated the relationship between seismicity and the Moho depth in the context of an overview of the earth crust under China, and likewise Deng et al. (2012) when studying the segmentation of the Tancheng–Lujiang fault and its implications to the lithosphere evolution in East China.

In order to look into this relationship, we calculated the average Moho depth (H) and the average focal depth (d) in relation with the four tectonic units under study. The method to obtain the parameter H consisted of interpolating the Moho depth on a regular grid and calculate the average, whereas the method to obtain the parameter d consisted of adding all focal depths and then divide the result by the number of data. To partly overcome the error in earthquake location and provide a mean value of reference, the lower bound of the seismicity (L) was defined as the depth above which is located 90% of the foci of the earthquakes (we discarded deep earthquakes with depth greater than 150 km). In turn we defined the ratio $\alpha = d/H$ and the ratio $\beta = L/H$, which are two new parameters that allow us to delve into this topic (Zhang et al., 2002). The results are shown together in Table 1. The average focal depth was found at 10 km, 12 km, 15 km and 13 km in Southeast China, North and Northeast China, Northwest China and Tibet, respectively. For these same tectonic blocks the average

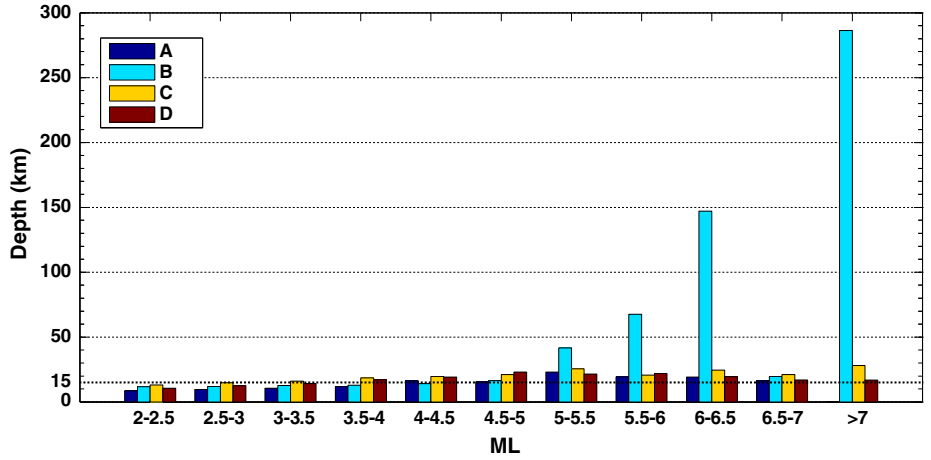

Fig. 11. Magnitude versus focal depth. The data correspond to the earthquakes occurred during the period January 1980–January 2013. Key to columns: A, Southeast China; B, North and Northeast China; C, Northwest China; D, Tibetan Plateau.

Table 1
Number of earthquakes, Moho depth (H), average focal depth (d) and lower bound of the seismicity (L) for each of the tectonic units considered in this study. The ratios $\alpha = d/H$ and $\beta = L/H$ are also included.

Regions	A	B	C	D
No. of earthquakes	14,434	27,985	27,962	27,717
Moho depth H (km)	35	38	51	65
Av. focal depth d (km)	10	12	15	13
Ratio $\alpha = d/H$	0.30	0.32	0.29	0.20
Lower bound seismicity L (km)	21	41	30	36
Ratio $\beta = d/H$	0.64	1.08	0.59	0.55

Notation: A, Southeast China; B, North and Northeast China; C, Northwest China; D, Tibetan Plateau.

Moho depth was found at 35 km, 38 km, 51 km and 65 km, respectively. From this it follows that d is always less than H and that comparatively the largest average focal depth (15 km) is in Northwest China. In addition, $\alpha = 0.3$ could be taken as reference value to estimate the place where a great part of the earthquakes occur. However, the parameter L, based on 90% of the detected earthquakes, takes the values 21 km, 41 km, 30 km and 36 km (Table 1). The lower bound of the seismicity L is also less than H and therefore the ratio β is less than 1; but L is exceptionally deeper than the Moho depth in North China (41 km versus 38 km) and this makes the ratio β to be greater than 1 unlike what happens in the rest of the areas.

5.2. Seismogenic structure

In the continents, and away from subduction zones, seismicity is usually concentrated in the top 20 km of the crust, whereas the lower crust is generally, although not always, considerably less active or even completely aseismic (Molnar and Chen, 1983). Below we analyze the seismogenic structure (hypocenters, seismic energy released) related to the crustal P-wave velocity for the tectonic regions that make up East Asia. The same method has been applied in recent studies (Deng et al., 2012; Wu and Zhang, 2012; Zhang et al., 2011c, 2013a). To illustrate the procedure, in Fig. 12a we can see the distribution of hypocenters of shallow earthquakes (red full circles whose size is proportional to its magnitude) in a sample of lithospheric column of 60 km depth; the number at the bottom of the graph indicates the amount of seismic events counted. The method requires the calculation of the seismic

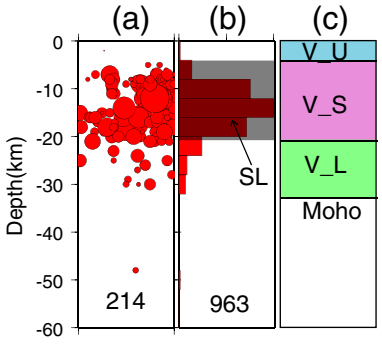

Fig. 12. (a) Hypocenters of shallow earthquakes (red circles) down to a depth of 60 km (left scale); the number at the bottom of the graph indicates the number of seismic events. (b) Distribution of the logarithm of the seismic energy log E/Emax represented by horizontal filled bars (in red color); the number at the bottom of the graph indicates the maximum value of the energy (Emax) used for normalization; SL means seismogenic layer (shaded area), i.e. where most of the seismic energy is released. (c) Sketch of the three parts of the crust: VU stands for the average velocity in the upper layer, VS is synonymous of average velocity in the seismogenic layer and VL means average velocity in the lower layer. The earthquake data for the period January 1980–January 2013 were taken from the catalogue edited by the China Earthquake Network Center.

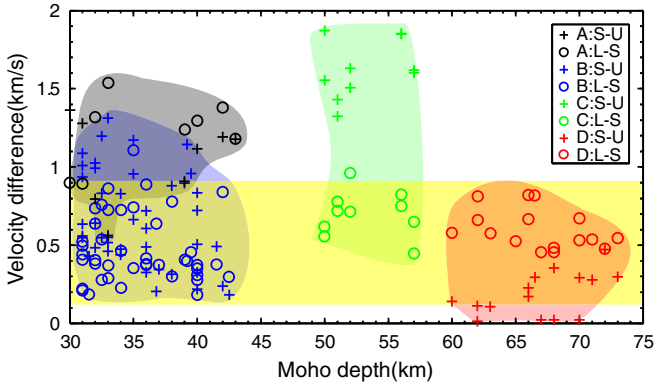

Fig. 13. Plot showing the differences in seismic velocity versus the Moho depth in relation to the four tectonic units in which East Asia has been divided: A, Southeast China; B, North and Northeast China; C, Northwest China; D, Tibetan Plateau. Key to symbols: S–U, velocity (on average) of the seismogenic layer minus velocity of the upper layer; L–S: velocity (on average) of the lower layer minus velocity of the seismogenic layer. The shaded areas contain the values found for each of the tectonic units considered in this study. The horizontal broad band (shaded in yellow color) represents the variation range between 0.1 and 0.9 km/s of most of the velocity differences found.

energy (E) which to this end is computed from the earthquake magnitude (M_S) using the relationship $\log E = 11.8 + 1.5\, M_S$ (Panza and Raykova, 2008; Richter, 1958). The value of M_S is either taken directly from the catalog edited by the China Earthquake Network Center (CENC) or calculated from currently available relationships between M_S and ML, when the event size is expressed as local ML magnitude in the CENC catalog. In China mainland the surface-wave M_S magnitude can be approximated by local ML magnitude through the relationship $M_S = 1.13 \times ML - 1.08$ (Fu and Liu, 1980) for the calculation of the seismic energy (Panza and Raykova, 2008). In Fig. 12b we have plotted the statistics of the logarithm of the seismic energy, log E/Emax, versus depth by means of a histogram of horizontal filled bars. The maximum value of the energy Emax used for normalization is given at the bottom of the column. To construct this figure the earthquakes were taken at 4 km depth intervals. In this context, seismogenic layer is the layer wherein 80% of the seismic energy is released, while any other structure in the crust depicts the non-seismogenic layer (Deng et al., 2012). The seismogenic layer is denoted by its acronym SL and appears like a shaded area in Fig. 12b. With the constraints inherent to the Moho, here we define the part of the crust above the seismogenic layer as 'upper layer' and the part beneath the seismogenic layer as 'lower layer'. The respective average P-wave velocities corresponding to these three layers are: VU for the upper layer, VS for the seismogenic layer and VL for the lower layer, as shown schematically in Fig. 12c.

With the purpose of investigating the link between the seismogenic structure and the P-wave velocity of the crust in East Asia, we selected the same deep seismic profiles as Zhang et al. (2013a) to the knowledge of velocity data. Based on the above description of seismogenic structure, we calculated the difference in velocity between the upper and seismogenic layers, and likewise between the lower and seismogenic layers. Such a difference in velocity is the expression of the Lamé parameters of the crustal layers, which in turn are related to the physical mechanism of earthquakes generation (Fitzenz and Miller, 2001; Tsuruoka et al., 1995). Fig. 13 shows these differences versus Moho depth for the four tectonic units of reference. At first glance all blocks present remarkable dissimilarities in terms of velocity contrasts. The Moho depth in Southeast China varies from 30 to 44 km, and the velocity differences with the seismogenic layer go from ~0.8 to 1.5 km/s, thus revealing clear structural differences among the three layers in this region. In North and Northeast China the Moho depth is scaled as in Southeast China, while the velocity differences with the seismogenic layer vary within a wider interval from 0.2 km/s to 1.3 km/s; nevertheless a large part of this velocity contrast could be due to the comparably larger

size of the region. The Moho in Northwest China stays at a relatively constant depth of about 50–57 km, but the larger velocity differences, 0.5–1.9 km/s, can be the response of the complex geodynamics of the region. As expected, the Tibetan Plateau presents the deepest undulating Moho, 60–73 km depth, but now the differences in velocity are below 0.9 km/s, which means the upper and lower crustal layers have roughly the same characteristic velocity and consequently similar (although not equal) earthquake generating capacity as the seismogenic layer.

Other features derive from the results: in the Tibetan Plateau the velocity differences between the seismogenic layer and the upper layer are smaller than those between the lower layer and the seismogenic layer; however all the opposite happens in North China. These discrepancies suggest a smaller capacity of the upper crustal layer to generate earthquakes when compared to the lower layer in Northwest China, as shown in Fig. 11 of Zhang et al. (2013a).

Since most of the velocity differences come to fall within the range 0.1–0.9 km/s (yellow shaded band in the illustration), this last value (0.9 km/s) may be understood as an upper threshold for a less generation of earthquakes in the crust interior. A difference in seismic velocity bigger than this range would mean that the layer has an earthquake generating capacity lesser than the seismogenic layer, as happens in South China and Northwest China; while a smaller difference in velocity would imply that the layer has a comparable seismogenic capacity, such as happens in Tibet.

Alternatively, there are other classic parameters to study the seismogenic structure as Vp, Vs and the ratio Vp/Vs. Zhao et al. (2000) found that big earthquakes in the crust (M 5.7–8.0, depth 0–20 km) from 1885 to 1999 in Japan, occurred in or around low-velocity zones, or even in boundary areas between low- and high-velocity zones revealed by seismic tomography. They suggested that the low-velocity zones may represent weak sections of the seismogenic crust and may be caused by magma chambers or fluids resulting from the dehydration of the subducting oceanic slab. Hauksson and Haase (1997) found that four $M > 5.9$ earthquakes in the Los Angeles basin area occurred in or near high-velocity zones. They interpreted that the high-velocity zones form the upper block of a thrust fault or a thin-skinned structure; that is, that the ruptures happened at the boundary between high- and low-velocity zones as shown in Fig. 13 of Hauksson and Haase (1997). Hence their results for southern California are consistent with the observations in Japan by Zhao et al. (2000).

In the Sichuan–Yunnan region, Huang et al. (2003) also found that large fault zones and most of the big crustal earthquakes (in particular those with $M > 5.0$) are located at the border between high- and low-velocity zones of the crust.

Qi et al. (2006) revealed a rather heterogeneous P- and S-velocity structure in the Chinese capital region. They found shallow velocity anomalies consistent with the main surface geological features, and also that strong earthquakes often occur in the transition between low and high velocity zones, and in zones with low Poisson's ratio too. Low-velocity anomalies together with a high Poisson's ratio were also found near the earthquake hypocenters.

Vp, Vs and the ratio Vp/Vs are affected when the earth materials seem to be less consolidated, such as seismic tomography reveals clearly, and this plays an important role in the earthquake generation and triggering processes (Huang et al., 2002; Qi et al., 2006; Zhao et al., 2011). This is in line with the difference in seismic velocity respect to that of the seismogenic layer.

6. Conclusions

We have conducted a mapping of the Moho from the data supplied by deep seismic profiles performed in East Asia. This has allowed us observe the changes in the Moho depth with relation to the four large tectonic blocks that make up the Chinese continent, namely: Southeast China, North and Northeast China, Northwest China and Tibetan Plateau. Second, we have analyzed the seismicity pattern affecting these regions. Third, we have determined the regional seismogenic structure in function of the released seismic energy.

The results obtained lead to the following conclusions:

(1) The crust–mantle discontinuity varies considerably from one to another tectonic province and lies at different depths as consequence of the strongly changing morphology that characterizes the vast study area with remarkable differences from each other places. The average thickness of the crust is 65 km in the Tibetan Plateau, but it can reach values close to 75 km and likely more. This mean value becomes about 35 km in South China, 38 km in North and Northeast China and 51 km in Northwest China. The crust is thinner in the continental margin and sea area where the Moho depth does not exceed 20–28 km.

(2) According to the focal mechanisms of the events spread across all zones, North and Northeast China are dominated by extensional deformation, unlike Northwest China that is affected by a compression regime. The margin of the Tibetan Plateau is under a convergent compressive regime, despite the deformation in the interior of Tibet is rather of extensional type. Most of the earthquakes have magnitude less than 4.0, are located in the uppermost 20 km of the crust, and only a few of the bigger events lie at deeper depths. The average focal depth is above the Moho and ranges between 10 km in Southeast China and 15 km in Northwest China. The ratio of the average focal depth to the Moho depth is approximately 0.3 and this value can be taken as reference to discriminate the places where a great part of the earthquakes occur. Likewise, the lower bound of the seismicity is always above the Moho, except for North and Northeast China.

(3) Most of the differences in velocity of the upper and lower crustal layers with respect to the seismogenic layer are within the range 0.1–0.9 km/s. A difference greater than 0.9 km/s would indicate a comparatively lower capacity to generate seismic events. In South China the discrepancy in seismic velocity stands above 0.8 km/s, which agrees with the lack of earthquakes in the region. Just the opposite happens in Tibet; so that it is possible argue that the upper and lower crustal layers have similar capacity to generate earthquakes, although it is true that a lesser extent in the upper layer (discrepancy of less than 0.4 km/s). In Northwest China the upper layer (discrepancy greater than 1.3 km/s) exhibits a less capacity for generating seismic energy when compared to the lower layer. Lastly, in North and Northeast China, leaving aside the dispersion of results because of the larger size of this region, all the crust has a comparable seismogenic capacity.

Acknowledgments

The authors want to thank all those people who participated in deep seismic soundings for more than half a century in China; and also to thank Jing Wu, Institute of Geology and Geophysics, Chinese Academy of Sciences, for her help during this work. We appreciate the helpful observations and constructive suggestions from Professor M. Santosh and two anonymous reviewers, which led to significantly improve the manuscript. The present work takes advantage of the Collaboration Agreement between the Institute of Geology and Geophysics, Chinese Academy of Sciences, Beijing, and the University of Zaragoza, Spain. This research benefited from the support of the National Nature Science Foundation of China (grants 90914012, 41130419, 41374064) and the Ministry of Land and Resources (SINOPROBE-02-02, SINOPROBE-03-02).

Appendix A. Supplementary data

Supplementary data to this article can be found online at http://dx.doi.org/10.1016/j.tecto.2013.11.008.

References

Chang, C.F., Pan, Y.S., 1981. A brief discussion on the tectonic evolution of the Qinghai–Xizang plateau. Geological and Ecological Studies of the Qinghai–Xizang (Tibet) Plateau, vol. 1. Science Press, Beijing 1–18.

Chang, C.F., Nansheng, C., Coward, M.P., Wanming, D., Dewey, J.F., Gansser, A., Harris, N.B.W., Chengwei, J., Kidd, W.S.F., Leeder, M.R., 1986. Preliminary conclusions of the Royal Society and Academia Sinica 1985 Geotraverse of Tibet. Nature 323, 501–507.

Chen, X.B., Zhang, J.F., Tang, R.Y., 2001. Introduction of depth map of Moho under China and its surrounding areas (1:15000000). Seismology Press, Beijing (in Chinese)

Chen, Y., Badal, J., Hu, J., 2009. Love and Rayleigh wave tomography of the Qinghai–Tibet Plateau and surrounding areas. Pure Appl. Geophys. 167 (10), 1171–1203. http://dx.doi.org/10.1007/s00024-009-0040-1.

Cui, Z.Z., Li, Q.S., Wu, C.D., Yin, Z.X., Liu, H.B., 1995. The crustal structure and deep tectonics along Golmud–Ejinaqi transect. Chin. J. Geophys. 38 (Suppl. II), 15–28 (in Chinese with abstract in English).

Deng, Y., Fan, W., Zhang, Z., Badal, J., 2012. Geophysical evidence on segmentation of the Tancheng–Lujiang fault and its implications on the lithosphere evolution in East China. J. Asian Earth Sci. http://dx.doi.org/10.1016/j.jseaes.2012.11.006.

Deng, Y., Zhang, Z., Badal, J., Fan, W., 2014. 3-D density structure under South China constrained by seismic velocity and gravity data. Tectonophysics 627, 159–170.

Ekström, G., Nettles, M., Dziewonski, A., 2012. The global CMT project 2004–2010: Centroid-moment tensors for 13,017 earthquakes. Phys. Earth Planet. Inter. 200–201, 1–9.

Feng, R., 1985. Crustal thickness and density distribution of upper mantle in China (results from 3D gravitational inversion). Acta Seismol. Sin. 7, 143–157 (in Chinese with abstract in English).

Fitzenz, D.D., Miller, S.A., 2001. A forward model for earthquake generation on interacting faults including tectonics, fluids, and stress transfer. J. Geophys. Res. Solid Earth 106 (B11), 26689–26706 (1978–2012).

Foster, A.N., Jackson, J.A., 1998. Source parameters of large African earthquakes, implications for crustal rheology and regional kinematics. Geophys. J. Int. 134 (2), 422–448.

Fu, S.F., Liu, B.C., 1980. Seismology. Beijing University Press.

Gao, R., Lu, Z., Li, Q., Guan, Y., Zhang, J., He, R., Huang, L., 2005. Geophysical survey and geodynamic study of crust and upper mantle in the Qinghai–Tibetan Plateau. Episodes 28 (4), 263–273.

Geiger, L., 1912. Probability method for the determination of earthquake epicenters from the arrival time only. Bull. St. Louis Univ. 8 (1), 56–71.

Gilbert, F., 1971. Excitation of the normal modes of the Earth by earthquake sources. Geophys. J. Int. 22 (2), 223–226.

Gorman, A.R., Clowes, R.M., Ellis, R.M., Henstock, T.J., Spence, G.D., Keller, G.R., Levander, A., Snelson, C.M., Burianyk, M.J., Kanasewich, E.R., 2002. Deep Probe: imaging the roots of western North America. Can. J. Earth Sci. 39 (3), 375–398.

Grad, M., Tiira, T., 2009. The Moho depth map of the European Plate. Geophys. J. Int. 176 (1), 279–292.

Hauksson, E., Haase, J.S., 1997. Three-dimensional VP and VP/VS Velocity Models of the Los Angeles basin and central Transverse Ranges, California. J. Geophys. Res. 102 (B3), 5423–5453.

Huang, J., Zhao, D., Zheng, S., 2002. Lithospheric structure and its relationship to seismic and volcanic activity in southwest China. J. Geophys. Res. 107 (B10), 13–14 (ESE 13-11-ESE).

Huang, J., Song, X., Wang, S., 2003. Fine structure of Pn velocity beneath the Sichuan-Yunnan region. Sci. Chin. (Series D: Earth Sciences) 46 (2), 201–209.

Jahn, B., Nyquist, L.E., 1976. Crustal evolution in the early earth–moon system: constraints from Rb–Sr studies. In: Windley, B.F. (Ed.), The Early History of the Earth. John Wiley and Sons Co., pp. 55–76.

Jahn, B., Wu, F., Chen, B., 2000. Granitoids of the Central Asian Orogenic Belt and continental growth in the Phanerozoic. Trans. R. Soc. Edinb. 91, 181–194.

Jia, S.X., Zhang, X.K., 2005. Crustal structure and comparison of different tectonic blocks in North China. Chin. J. Geophys. 48 (3), 611–620 (in Chinese with abstract in English).

Klein, F.W., 2002. User's guide to HYPOINVERSE-2000: a Fortran program to solve for earthquake locations and magnitudes. USGS Open File Report 02-171, Version 1.0. 1–123.

Laske, G., Masters,, G., Reif, C., 2001. CRUST2.0—a new global crustal model at 2 × 2 degrees. (http://mahi.ucsd.edu/Gabi/crust2.html).

Lei, J., Zhao, D., 2005. P-wave tomography and origin of the Changbai intraplate volcano in Northeast Asia. Tectonophysics 397 (3), 281–295.

Li, Z.X., 1994. Collision between the North and South China blocks: a crustal detachment model for suturing in the region east of the Tanlu fault. Geology 22 (8), 739–742.

Li, Q.S., Gao, R., Lu, D.Y., Li, J.W., Fan, J.Y., Zhang, Z.Y., Liu, W., Li, Y.K., Yan, Q.R., Li, D.X., Team Wide Angle, 2001. Tarim underthrust beneath western Kunlun: evidence from wide-angle seismic sounding. J. Asian Earth Sci. 18, 281–292.

Li, S., Mooney, W., Fan, J., 2006. Crustal structure of mainland China from deep seismic sounding data. Tectonophysics 420 (1–2), 239–252.

Li, Q., Gao, R., Wu, F.T., Guan, Y., Ye, Z., Liu, Q., Kuo-Chen, H., He, R., Li, W., Shen, X., 2013. Seismic structure in the southeastern China using teleseismic receiver functions. Tectonophysics 606, 24–35.

Liu, R.X., 1992. Geochronology and geochemistry of cenozoic volcanic rocks of China. Geological Publishing House, Beijing.

Liu, Y.L., Zheng, J.C., Jiao, L.X., 1994. A study of deep structure of China and its geological significance. advances in solid earth geophysics in China. Honor of Professor Zeng Rongsheng's 70th Birthday. Ocean Press, Beijing, pp. 113–119 (in Chinese).

Liu, C.Q., Fang, S.M., Li, C.F., 1996. Joint gravity-seismic interpretation for Yingxian–Zibo profile. Seismolog. Geol. 18 (4), 369–374 (in Chinese with abstract in English).

Lloyd, S., van der Lee, S., França, G.S., Assumpção, M., Feng, M., 2010. Moho map of South America from receiver functions and surface waves. J. Geophys. Res. Solid Earth 115 (B11) (1978–2012).

Ma, X., 1989. Lithosphere and Dynamics Atlas of China. Chinese State Seismological Bureau, China Cartographic Publishing House, Beijing.

Maggi, A., Jackson, J.A., McKenzie, D., Priestley, K., 2000. Earthquake focal depths, effective elastic thickness, and the strength of the continental lithosphere. Geology 28, 495–498.

Molnar, P., Chen, W.P., 1983. Focal depths and fault plane solutions of earthquakes under the Tibetan Plateau. J. Geophys. Res. 88 (B2), 1180–1196.

Panza, G.F., Raykova, R.B., 2008. Structure and rheology of lithosphere in Italy and surrounding. Terra Nova 20 (3), 194–199.

Prodehl, C., Kennett, B., Artemieva, I.M., Thybo, H., 2013. 100 years of seismic research on the Moho. Tectonophysics 609, 9–44.

Qi, C., Zhao, D.P., Chen, Y., Chen, Q.F., Wang, B.S., 2006. 3-D P and S wave velocity structures and their relationship to strong earthquakes in the Chinese capital region. Chin. J. Geophys. 49 (3), 805–815 (in Chinese with abstract in English).

Richter, C.F., 1958. Elementary seismology. W.H. Freeman & Co., San Francisco.

Santosh, M., Zhao, D.P., Kusky, T., 2010. Mantle dynamics of the Paleoproterozoic North China Craton: a perspective based on seismic tomography. J. Geodyn. 49 (1), 39–53.

Santosh, M., Liu, S.J., Tsunogae, T., Li, H.J., 2012. Paleoproterozoic ultrahigh-temperature granulites in the North China Craton: Implications for tectonic models on extreme crustal metamorphism. Precambrian Res. 222–223, 77–106.

Sengör, A., Burtman, V., 1993. Evolution of the Altaid tectonic collage and Palaeozoic crustal growth in Eurasia. Nature 364, 299–307.

Sengör, A.M.C., Natal'In, B.A., Burtman, V.S., 1996. Turkic-type orogeny and its role in the making of the continental crust. Annu. Rev. Earth Planet. Sci. 24, 263–337.

Sherrington, H.F., Zandt, G., Frederiksen, A., 2004. Crustal fabric in the Tibetan Plateau based on waveform inversions for seismic anisotropy parameters. J. Geophys. Res. 109, B02312.

Sipkin, S.A., 1994. Rapid determination of global moment-tensor solutions. Geophys. Res. Lett. 21 (16), 1667–1670.

Song, Z.H., An, C.Q., Chen, G.Y., Chen, L.H., Zhuang, Z., Fu, Z.W., 1994. 3D S-wave velocity structure of the crust and upper mantle. Sci. China, Ser. B 37 (1), 104–116.

Teng, J.W., 1979. Geophysical investigations of the Earth's crust and upper mantle in China. Chin. J. Geophys. (Acta Geol. Sin.) 22, 346–350 (in Chinese with abstract in English).

Teng, J.W., Xiong, S.B., Sun, K.Z., 1981. Explosive seismology for crust and upper mantle structure and velocity distribution beneath Danxiong–Yadong areas, Xizang Plateau. Chin. J. Geophys. (Acta Geol. Sin.) 24 (2), 155–170 (in Chinese with abstract in English).

Teng, J.W., Wang, Q.S., Liu, Y.L., 1982. Basic pattern of crustal structure in China. Pet. Geophys. Prospect. 2, 14–20 (in Chinese).

Teng, J.W., Sun, K.Z., Xiong, S.B., Yin, Z.X., Chen, L.F., 1983. Deep seismic reflection waves and structure of the crust from Dangxung to Yadong on the Xizang plateau (Tibet). Phys. Earth Planet. Inter. 31 (4), 293–306.

Teng, J.W., Yin, Z.X., Xiong, S.B., 1985a. Crustal structure and velocity distribution beneath the Serlin–Peng–Naqu–Suo region in the Northern Xizang (Tibet) Plateau. Chin. J. Geophys. (Acta Geol. Sin.) 28, 28–42 (in Chinese with abstract in English).

Teng, J.W., Xiong, S.B., Yin, Z.X., 1985b. Structure of the crust and upper mantle pattern and velocity distribution characteristics in the northern region of the Himalayan mountain region. J. Phys. Earth 33 (3), 157–171.

Teng, J., Zeng, R., Yan, Y., Zhang, H., 2003. Depth distribution of Moho and tectonic framework in eastern Asian continent and its adjacent ocean areas. Sci. China Ser. D Earth Sci. 46 (5), 428–446.

Teng, J., Zhang, Z., Zhang, X., Wang, C., Gao, R., Yang, B., Qiao, Y., Deng, Y., 2013. Investigation of the Moho discontinuity beneath the Chinese mainland using deep seismic sounding profiles. Tectonophysics 609, 202–216.

Thybo, H., Artemieva, I.M., 2013. Moho and magmatic underplating in continental lithosphere. Tectonophysics 608, 605–619.

Tsuruoka, H., Ohtake, M., Sato, H., 1995. Statistical test of the tidal triggering of earthquakes: contribution of the ocean tide loading effect. Geophys. J. Int. 122 (1), 183–194.

Waldhauser, F., Ellsworth, W.L., 2000. A double-difference earthquake location algorithm: method and application to the northern Hayward fault, California. Bull. Seismol. Soc. Am. 90 (6), 1353.

Wang, Q.S., 1985. Distribution framework of crustal thickness under Asian continent and discussion of crustal tectonic features. Tectonic Geol. Rev. 4, 13–23 (in Chinese).

Wang, Y., Fan, W., Zhang, G., Zhang, Y., 2013. Phanerozoic tectonics of the South China Block: key observations and controversies. Gondwana Res. 23 (4), 1273–1305.

Wu, J., Zhang, Z.J., 2012. Spatial distribution of seismic layer, crustal thickness, and Vp/Vs ratio in the Permian Emeishan mantle plume region. Gondwana Res. 22 (1), 127–139.

Xiao, W.J., Windley, B.F., Hao, J., Zhai, M.G., 2003. Accretion leading to collision and the Permian Solonker suture, Inner Mongolia, China, termination of the Central Asian orogenic belt. Tectonics 22, 1069. http://dx.doi.org/10.1029/2002TC001484.

Xiao, W.J., Zhang, L.C., Qin, K.Z., Sun, S., Li, J.L., 2004. Paleozoic accretionary and collisional tectonics of the Eastern Tianshan (China): implications for the continental growth of central Asia. Am. J. Sci. 304, 370–395.

Xiao, W., Kusky, T., 2009. Geodynamic processes and metallogenesis of the Central Asian and related orogenic belts: Introduction. Gondwana Res. 16 (2), 167–169.

Xu, T., Xu, G., Gao, E., Li, Y., Jiang, X., Luo, K., 2006. Block modeling and segmentally iterative ray tracing in complex 3D media. Geophysics 71 (3), T41–T51.

Xu, T., Zhang, Z., Gao, E., Xu, G., Sun, L., 2010. Segmentally iterative ray tracing in complex 2D and 3D heterogeneous block models. Bull. Seismol. Soc. Am. 100 (2), 841–850.

Xue, X.K., Wang, T.D., Zhang, H.Q., Zhang, J.L., 2006. The deep crust features of the Junggar basin and petroleum exploration targets. Nat. Gas Ind. 26 (10), 37–41 (in Chinese with abstract in English).

Yang, H., Hu, J., Hu, Y., Duan, Y., Li, G., 2013. Crustal structure in the Tengchong volcanic area and position of the magma chambers. J. Asian Earth Sci. 73, 48–56.
Yin, X.H., Shi, Z.H., Liu, Z.B., 1990. Basical feature of regional gravitation field for China Continent. Seismol. Geol. 2 (4), 69–75 (in Chinese with abstract in English).
Yin, Z.X., Lai, M.H., Xiong, S.B., Liu, H.B., Teng, J.W., Kong, X.R., 1999. Crustal structure and velocity distribution from deep seismic sounding along the profile of Lianxian–Boluo–Gangkou in South China. Chin. J. Geophys. 42 (3), 383–392 (in Chinese with abstract in English).
Yin, A., Harrison, T.M., 2000. Geologic evolution of the Himalayan–Tibetan orogen. Annu. Rev. Earth Planet. Sci. 28, 211–280.
Zeng, R.S., Gan, R.J., 1961. Reflected waves from crustal interface in western Chaitamu Basin. Chin. J. Geophys. (Acta Geol. Sin.) 10 (1), 120–125 (in Chinese with abstract in English).
Zhai, M.G., Windley, B.F., Kusky, T.M., Meng, Q.R. (Eds.), 2007. Mesozoic subcontinental lithospheric thinning under eastern Asia. Geological Society, Special Publications, London.
Zhang, Z.M., Liou, J.G., Coleman, R.G., 1984. An outline of the plate tectonics of China. Geol. Soc. Am. Bull. 95, 295–312.
Zhang, G.M., Wang, S.Y., Li, L., Zhang, X.D., Ma, H.S., 2002. Focal depth research of earthquakes in mainland China: implication for tectonics. Chin. Sci. Bull. 47 (9), 663–668 (in Chinese).
Zhang, Z., Klemperer, S.L., 2005. West–east variation in crustal thickness in northern Lhasa block, central Tibet, from deep seismic sounding data. J. Geophys. Res. 110, B09403.
Zhang, Z., Badal, J., Li, Y., Chen, Y., Yang, L., Teng, J., 2005. Crust–upper mantle seismic velocity structure across Southeastern China. Tectonophysics 395 (1), 137–157.
Zhang, Z.J., Wang, Y.H., 2007. Crustal structure and contact relationship revealed from deep seismic sounding data in South China. Phys. Earth Planet. Inter. 165, 114–126.
Zhang, Z., Zhang, X., Badal, J., 2008. Composition of the crust beneath southeastern China derived from an integrated geophysical data set. J. Geophys. Res. 113, B04417. http://dx.doi.org/10.1029/20006JB004503.
Zhang, Z., Teng, J., Badal, J., Liu, E., 2009. Construction of regional and local seismic anisotropy structures from wide-angle seismic data: crustal deformation in the southeast of China. J. Seismol. 13, 241–252. http://dx.doi.org/10.1007/s10950-008-9124-0.
Zhang, C.J., Zhang, X.D., Miao, C.L., Ding, Q.Q., Zhang, A.W., Lin, J., 2011a. The analysis of the theoretical error in measuring the focal depth of near earthquake. Earthq. China 26 (2), 156–163 (in Chinese).
Zhang, Z., Deng, Y., Teng, J., Wang, C., Gao, R., Chen, Y., Fan, W., 2011b. An overview of the crustal structure of the Tibetan Plateau after 35 years of deep seismic soundings. J. Asian Earth Sci. 40 (4), 977–989.
Zhang, Z., Yang, L., Teng, J., Badal, J., 2011c. An overview of the earth crust under China. Earth Sci. Rev. 104, 143–166. http://dx.doi.org/10.1016/j.earscirev.2010.10.003.
Zhang, Z., Klemperer, S., Bai, Z., Chen, Y., Teng, J., 2011d. Crustal structure of the Paleozoic Kunlun orogeny from an active-source seismic profile between Moba and Guide in East Tibet, China. Gondwana Res. 19 (4), 994–1007.
Zhang, Z., Xu, T., Zhao, B., Badal, J., 2012. Systematic variations in seismic velocity and reflection in the crust of Cathaysia: New constraints on intraplate orogeny in the South China continent. Gondwana Res. http://dx.doi.org/10.1016/j.gr.2012.05.018.
Zhang, S.B., Zheng, Y.F., 2013. Formation and evolution of Precambrian continental lithosphere in South China. Gondwana Res. 23 (4), 1241–1260.
Zhang, Z., Deng, Y., Chen, L., Wu, J., Teng, J., Panza, G., 2013a. Seismic structure and rheology of the crust under mainland China. Gondwana Res. 23 (4), 1455–1483.
Zhang, Y.C., Shi, G.R., Shen, S.Z., 2013b. A review of Permian stratigraphy, palaeobiogeography and palaeogeography of the Qinghai–Tibet Plateau. Gondwana Res. 24 (1), 55–76.
Zhao, G.C., Cawood, P.A., 1999. Tectonothermal evolution of the Mayuan assemblage in the Cathaysia Block; implications for Neoproterozoic collision-related assembly of the South China Craton. Am. J. Sci. 299, 309–339.
Zhao, D., Ochi, F., Hasegawa, A., Yamamoto, A., 2000. Evidence for the location and cause of large crustal earthquakes in Japan. J. Geophys. Res. 105 (B6), 13579–13594.
Zhao, G., Wilde, S.A., Cawood, P.A., Sun, M., 2001. Archean blocks and their boundaries in the North China Craton: lithological, geochemical, structural and P–T path constraints and tectonic evolution. Precambrian Res. 107, 45–73.
Zhao, G.C., Sun, M., Wilde, S.A., Li, S., 2003. Assembly, accretion and breakup of the paleo-Mesoproterozoic Columbia supercontinent: records in the North China Craton. Gondwana Res. 6, 417–434.
Zhao, D., Yu, S., Ohtani, E., 2011. East Asia: seismotectonics, magmatism and mantle dynamics. J. Asian Earth Sci. 40 (3), 689–709.
Zhao, B., Zhang, Z., Bai, Z., Badal, J., Zhang, Z., 2013a. Shear velocity and *Vp/Vs* ratio structure of the crust beneath the southern margin of South China continent. J. Asian Earth Sci. 62, 167–179. http://dx.doi.org/10.1016/j.jseaes.2012.08.013.
Zhao, B., Bai, Z., Xu, T., Zhang, Z., Badal, J., 2013b. Lithological model of the South China crust based on integrated geophysical data. J. Geophys. Eng. 10. http://dx.doi.org/10.1088/1742-2132/10/2/025005.
Zhou, X., Li, W., 2000. Origin of Late Mesozoic igneous rocks in Southeastern China: implications for lithospheric subduction and underplating of mafic magmas. Tectonophysics 326, 269–287.
Zhu, J.S., Yan, Z.J., Yao, Y.F., 1996. Depth map of Moho discontinuity. geophysical map collections in China. Geology Press, Beijing 81–82 (1996).